Intra-Mode Squeezing in the Quantum Optical Frequency Comb

A Thesis presented to the Graduate Faculty of the University of Virginia in Candidacy for the Degree of Masters of Science in Physics

by

Benjamin Godek

University of Virginia
November 28, 2017

On my honor as a university student, on this assignment I have neither given nor received aid as defined by the Honor Guidelines for Papers in Science, Technology, and Society Courses.

(Full Signature)

Science, Technology, and Society Advisor-Olivier Pfister (Signature)

Abstract

This thesis demonstrates the presence of two-mode squeezing within a broadband squeezed light field generated by an OPO pumped just below threshold. Past experiments have confirmed the existence of this phenomenon, but we have demonstrated the technique over an approximately 1 MHz frequency range, with a highly tunable measurement technique. Through the use of a two-frequency local oscillator generated by a double sideband modulation of an EOM, we are able to measure many two-mode squeezed fields within the spectrum of one OPO output mode. Such a technique has great potential for observing larger, more densely packed optical cluster states, which could be used to construct a quantum computer.

Acknowledgements

I would like to personally thank my research advisor Olivier Pfister for his advice, knowledge, and support. I also thank my lab mates Zack Carson (UVA graduate student), Rajveer Nehra (UVA graduate student), Chung-Hun Chang (UVA graduate student), Ricky Elwell (undergraduate student), and Aye Win (Postdoc) for their hard work in the lab and many helpful conversations.

Contents

List of Figures

1 Introduction

Entanglement has fascinated physicists since the formulation of quantum mechanics. In their influential 1935 paper, Einstein, Podolsky, and Rosen recognized entanglement as a distinctively non-classical phenomenon, which could be used to test the validity of quantum mechanics as a “complete” description of nature [1]. Although the strangeness of entanglement led the aforementioned scientists to doubt quantum mechanics’ status as a complete description of nature, an understanding of entanglement has become crucial to the study of quantum systems. In particular, entanglement has been identified as a necessary component in realizing quantum computation. Quantum computing has been identified as a theoretically powerful tool, which could provide exponential speed-ups of some hard computational tasks [2], such as simulating quantum systems [3]. Cluster states, in which individual quantum bits (qubits) are connected via entangling gates provide a template for building a quantum computer [4, 5].

Constructing a cluster state based quantum computer would require the entanglement of multiple qubits; the larger the state, the more resources one has for quantum computing. Multi-partite entanglement has been engineered in trapped ion [6, 7] and photonic systems [8]. Cluster states can also be constructed using qmodes, which have a continuous spectrum, as opposed to the two-state system of a qubit. Quantum computing with qumodes is also referred to as continuous variable (CV) quantum computing. Scalability is a particular advantage of CV systems, which makes them attractive to use for building a large cluster state [9]. In 2014, a 60 mode cluster state with multipartite entanglement was created in the quantum optics group here at the University of Virginia. The state was constructed using the quantum optical frequency comb (QOFC) of a bimodally pumped optical parametric oscillator. The state was believed to be even larger(approximately 3,000 modes), but the limitations of the entanglement verification technique that was used prevented this from being proven [10]. Large scale optical entanglement has also been generated in the time domain [11], with modes separated temporally instead of being indexed by frequency, but the advantage of frequency space experiments is that the entire system is simultaneously available for use.

In this thesis, we report the generation of entangled frequency modes using the output of a single OPO and intra-mode entanglement. In the experiment upon which ours was based, correlations were observed between different eigenmodes of the OPO cavity [10]. Here, we observe bipartite entanglement within the bandwidth of one cavity mode. The number of modes available using this process is limited only by the bandwidth of the cavity mode, the linewidth of the OPO pump, and the bandwidth of the squeezing/entanglement verification measurement. Previous work in this area established the validity of the technique, but only one frequency separation between the two modes was used [12, 13, 14]. The method presented in this thesis successfully generates and verifies the presence of many entangled modes within a relatively narrow bandwidth. Using this method, a larger frequency entangled cluster state could be constructed in a relatively narrow bandwidth (compared to past experiments in the Pfister lab [10]).

2 Theory

2.1 Time Evolution in Quantum Mechanics

In quantum mechanics, there are three approaches to calculating how expectation values change in time, the Schrodinger picture, Heisenberg picture, and interaction or Dirac picture (this section is based heavily on Moran Chen's PhD thesis) [15]. A brief summary of the three will be useful for the analysis of this thesis.

In the Schrodinger picture, a state with Hamiltonian H follows the Schrodinger equation

$$i\hbar \frac{d\left|\Psi(t)\right\rangle}{dt} = H\left|\Psi(t)\right\rangle \tag{1}$$

If H is time independent we can postulate a solution $\left|\Psi(t)\right\rangle = U(t,t_0)\left|\Psi(t_0)\right\rangle$. Plugging this into the Schrodinger equation, we can derive

$$U(t,t_0) = e^{-i(t-t_0)H/\hbar} \tag{2}$$

As time evolves, the expectation value of an operator A goes as

$$\begin{aligned} &\left\langle\Psi(t)\right| A \left|\Psi(t)\right\rangle \\ =& \left\langle\Psi(t_0)U^\dagger\right| A \left|U\Psi(t_0)\right\rangle \end{aligned} \tag{3}$$

In the Schrodinger picture, the states evolve in time using a unitary evolution U, while the operators are constant in time.

In contrast, the Heisenberg picture attaches the time dependence of a quantum system to the operators instead of the states. The state in the Heisenberg picture is the same as the state at time $t = 0$ in the Schrodinger picture, and vice-versa for the operators. For both pictures to be valid, they must give the same measurement results, so we can set the expectation values in each picture equal

$$\begin{aligned} \left\langle\Psi_H(t)\right| A_H(t) \left|\Psi_H(t)\right\rangle &= \left\langle\Psi_H(t_0)\right| A_H(t) \left|\Psi_H(t_0)\right\rangle \\ &= \left\langle\Psi_S(t)\right| A_S(t) \left|\Psi_S(t)\right\rangle \\ &= \left\langle\Psi_S(t_0)U^\dagger\right| A_S(t_0) \left|U\Psi_S(t_0)\right\rangle \end{aligned} \tag{4}$$

From this we can see that $A_H(t) = U^\dagger A U$. Taking the derivative of A(t) (we will drop the subscript) and using Eq (22) we derive

$$\begin{aligned} &\frac{dA}{dt} = \frac{d(U^\dagger A(t_0)U)}{dt} \\ =& \frac{1}{i\hbar}(-U^\dagger H A(t_0)U + U^\dagger A(t_0) H U) \\ &= \frac{1}{i\hbar}[A(t), H] \end{aligned} \tag{5}$$

assuming that $A(t_0)$ is time independent and that U commutes with H. This gives us the Heisenberg equation

$$\frac{dA}{dt} = \frac{1}{i\hbar}[A(t), H] \tag{6}$$

which is often more convenient to use than the Schrodinger equation in quantum optics.

The third picture is called the interaction picture (sometimes the Dirac picture). It attaches time evolution to *both* the operators and the wave function. To do this, we break our Hamiltonian into two parts $H = H_0 + V$ where H_0 is a single system term, and V is a term that couples between multiple systems. In this paper, we will use the convention that the states evolve under H_0 and the operators evolve under V. We define

$$A_I(t) = U_0 A_H(t) U_0^\dagger = U_0 U^\dagger A_0 U U_0^\dagger \tag{7}$$

By taking the derivative with respect to time, we see that

$$\begin{aligned} \frac{dA_I}{dt} &= \frac{d(U_0 A_I U_0^\dagger)}{dt} \\ &= \frac{i}{\hbar}[A_I, H_0] + U_0 \frac{dA_H}{dt} U_0^\dagger \end{aligned} \tag{8}$$

By combining the Heisenberg equation with the second term of the above expression, we obtain

$$U_0 \frac{dA_H}{dt} U_0^\dagger = -\frac{i}{\hbar}[A_I, H_0] - \frac{i}{\hbar}[A_I, V] \tag{9}$$

This leads us directly to a clear analogue to the Heisenberg equation for V and A_I:

$$\frac{dA_I}{dt} = -\frac{1}{i\hbar}[A_I, V] \tag{10}$$

Now we must also account for the state evolution under H_0, which is straightforward. It must be the case that $|\Psi_I(t)\rangle = U_0 |\Psi_I(t_0)\rangle$. Now taking the derivative

$$\begin{aligned} \frac{d|\Psi_I(t)\rangle}{dt} &= \frac{dU_0}{dt}|\Psi_I(t_0)\rangle \\ &= -\frac{i}{\hbar} H_0 |\Psi_I(t_0)\rangle \end{aligned} \tag{11}$$

In the interaction picture, the state evolves as in the Schrodinger picture with the Hamiltonian H_0 and the operators evolve as in the Heisenberg picture with Hamiltonian V. The interaction picture is quite useful when applied to the optical parametric oscillator, so it will show up again later.

2.2 The Harmonic Oscillator

In quantum optics, a light field can be treated as a single quantum harmonic oscillator (this section is based heavily on Moran Chen's PhD thesis) [15]. The

Hamiltonian for a harmonic oscillator in one dimension is

$$H = \frac{p^2}{2m} + \frac{1}{2}m\omega^2 x^2 \tag{12}$$

where p is the momentum, m is the mass, and ω is the oscillation frequency $\omega = \sqrt{\frac{k}{m}}$ (k being the spring constant). Let us now define the dimensionless analogs to position and momentum

$$X = \sqrt{\frac{m\omega}{\hbar}}x \tag{13}$$

$$P = \sqrt{\frac{1}{m\omega\hbar}}p \tag{14}$$

These are known as the quadrature operators. When comparing the classical harmonic oscillator to the quantum system, we notice that the continuous energy spectrum of the classical oscillator gives way to discrete energy levels in the quantum case. The operators that move the system up or down one energy level are $a^\dagger$ the creation operator and its hermitian conjugate, a, the annihilation operator. When acting on a quantum state of the harmonic oscillator, they will respectively add or subtract one quanta of energy to the state. These quanta are known as phonons in the case of a mechanical oscillator, while quanta of the light field are called photons. These operators are related to the quadrature operators by

$$\begin{aligned} a &= \frac{1}{\sqrt{2}}(X + iP) \\ a^\dagger &= \frac{1}{\sqrt{2}}(X - iP) \end{aligned} \tag{15}$$

The Hamiltonian for the quantum harmonic oscillator written in terms of the creation/annihilation operators is

$$H = \hbar\omega(a^\dagger a + \frac{1}{2}) \tag{16}$$

This is also the Hamiltonian for a quantum light field in free space. Each photon added to the field adds energy of $\hbar\omega$, ω being the frequency of the field. The creation/annihilation operators are not hermitian, and therefore not observable, and they satisfy the commutation relation

$$[a, a^\dagger] = 1 \tag{17}$$

from which we derive that Q and P have the commutator

$$[X, P] = i \tag{18}$$

which leads to an uncertainty relation between X and P, as they are hermitian observables. In this thesis, I will use the notation $\Delta X = \sqrt{\langle X^2 \rangle - \langle X \rangle^2}$. The uncertainty relation is

$$\Delta X \Delta P \geq \frac{1}{2} \tag{19}$$

This is analogous the famous Heisenberg Uncertainty Principle, only formulated using our dimensionless operators. The amount of variance, or noise, in the quadrature operators is a crucial component of the proceedings discussed in this thesis.

2.3 Uncertainty of Quantum States of Light

Any quantum state of light must satisfy the uncertainty principle in its quadratures. To see how this works, let us examine the cases of a few types of quantum states (this section is based heavily on Moran Chen's PhD thesis) [15]. First, we will examine the photon number states, or Fock states. More precisely, Fock states are eigenstates of the photon number operator $N = a^\dagger a$. Fock states are written as $|n\rangle$, where n is an integer that denotes the number of photons in the state. They form an orthonormal basis, so $\langle n|n'|n|n'\rangle = \delta_{nn'}$. Fock states also have the following properties

$$\begin{aligned} a^\dagger |n\rangle &= \sqrt{n+1}\,|n+1\rangle \\ a\,|n\rangle &= \sqrt{n}\,|n-1\rangle \\ N\,|n\rangle &= n\,|n\rangle \end{aligned} \tag{20}$$

with the third relation being straightforward to derive from the first two. These relations can also be used to derive the expectation value and standard deviation of the quadrature operators X and P for the Fock state. Omitting the algebra, we arrive at

$$\langle n| X |n\rangle = \langle n| P |n\rangle = 0 \tag{21}$$

$$\Delta X = \Delta P = \sqrt{n + \frac{1}{2}} \tag{22}$$

Therefore we can see that for a Fock state, $\Delta X \Delta P = n + \frac{1}{2}$. For $n = 0$, commonly known as the vacuum state, the inequality is saturated, so that $\Delta X \Delta P = \frac{1}{2}$. This means that the vacuum state is a minimum uncertainty state.

Another noteworthy class of states are the coherent states. Coherent states are commonly referred to as "classical light" because they interact with beamsplitters and other optical elements in the way predicted by classical electromagnetism. They can be thought of as the quantum mechanical representation of a monochromatic plane wave, so they are a good representation of the output of lasers and other similar systems. We will write a coherent state as $|\alpha\rangle$, with α being a complex number analogous to the amplitude of the classical wave. Coherent states are generated by the displacement operator, defined as

$$D(\alpha) = e^{\alpha a^\dagger - \alpha^* a} \tag{23}$$

When we apply $D(\alpha)$ to the vacuum state, we must use the Baker-Campbell-Hausdorf formula

$$e^{A+B} = e^A e^B e^{-\frac{[A,B]}{2}} \tag{24}$$

which is applicable if A and B both commute with [A,B]. Using this, and the Taylor series for exponentials, we can derive that

$$|\alpha\rangle = D(\alpha)|0\rangle = e^{-\frac{|\alpha|^2}{2}} \sum_{n=0}^{\infty} \frac{\alpha^n}{\sqrt{n!}} |n\rangle \tag{25}$$

which is the representation of a coherent state in the Fock state basis. From this we can derive that a coherent state is an eigenstate of the annihilation operator

$$a|\alpha\rangle = \alpha|\alpha\rangle \tag{26}$$

Using this fact, it only requires a little bit of algebra to verify the results for the uncertainty of X and P in a coherent state:

$$\langle n| X |n\rangle = \frac{1}{\sqrt{2}}(\alpha + \alpha^*) \tag{27}$$

$$\langle n| P |n\rangle = \frac{-i}{\sqrt{2}}(\alpha - \alpha^*) \tag{28}$$

$$\Delta X = \Delta P = \frac{1}{\sqrt{2}} \tag{29}$$

This result shows that all coherent states are minimum uncertainty states, meaning the product of their variances always saturates the Heisenberg inequality. Now, we will progress to the states that are of interest in this thesis.

2.4 Squeezed States

The bulk of the analysis in this section is based on *Introductory Quantum Optics* by Knight and Gerry [16]. In general, we say that any state which has a measurable with variance less than the square root of the minimum uncertainty product is squeezed. In our case, this would mean that X or P would have variance less than 1/2. The conjugate variable then must have a larger variance, and is anti-squeezed. We will look at producing squeezed states in the same way as when we used a displacement operator on the vacuum state to produce coherent states. The operator which can produce squeezed states is

$$S(\xi) = exp[\frac{1}{2}(\xi^* a^2 - \xi a^{\dagger 2})] \tag{30}$$

Where $\xi = re^{i\theta}$, r being the squeezing parameter. If we apply this operator to the vacuum, our state (the squeezed vacuum state) is given by

$$|\xi\rangle = S|0\rangle \tag{31}$$

This state gives us the following values for the quadrature variances, if we set $\theta = 0$:

$$\Delta X = \frac{1}{\sqrt{2}} e^{-2r} \tag{32}$$

$$\Delta P = \frac{1}{\sqrt{2}} e^{2r} \tag{33}$$

By changing the value of θ we can tune which quadratures are squeezed and anti-squeezed, while r determines the amount of squeezing. We can also look how the squeezed vacuum state is written in terms of the photon number basis (again using the Baker-Campbell-Hausdorf formula):

$$|\xi\rangle = \frac{1}{\sqrt{\cosh(r)}} \sum_{m=0}^{\infty} (-1)^m \frac{\sqrt{(2m)!}}{2^m m!} e^{im\theta} \tanh^m(r) |2m\rangle \tag{34}$$

A notable feature of this state is that the sum contains only even number states. Now we'll look at two mode squeezing. Let's take modes a and b, and find an operator that produces a two mode squeezed state when applied to the two mode vacuum:

$$S_2 |0_a, 0_b\rangle \tag{35}$$

Now we define the superposition quadrature operators as

$$X' = \frac{1}{2^{3/2}} (a + a^\dagger + b + b^\dagger) \tag{36}$$

$$P' = \frac{1}{2^{3/2}} (a - a^\dagger + b - b^\dagger) \tag{37}$$

We want an operator that squeezes these quadratures, which are formed from the superposition of the creation and annihilation operators of two distinct modes of light. This operator takes the form

$$S_2(\xi) = exp(\xi^* ab - \xi a^\dagger b^\dagger) \tag{38}$$

Again, for $\theta = 0$ we get the following type of squeezing if we apply our two mode squeezing operator to the two mode vacuum state, which we can tune by changing θ:

$$\Delta X' = \frac{1}{\sqrt{2}} e^{-2r} \tag{39}$$

$$\Delta P' = \frac{1}{\sqrt{2}} e^{2r} \tag{40}$$

The two mode squeezed vacuum state is, in terms of the Fock basis

$$|\xi\rangle_2 = \frac{1}{\cosh(r)} \sum_{n=0}^{\infty} (-1)^n e^{in\theta} \tanh^n(r) |n, n\rangle \tag{41}$$

Note that the two modes always have the same number of photons. This means that the the two modes are entangled, as measuring the photon number of one will reveal the photon number of the other. In this paper, it is the entanglement of the two mode squeezed state that is ultimately of consequence.

Finally, we note that the squeezing operators $S(\xi)$ and $S_2(\xi)$ are simply unitary operators U that were covered in the section regarding time evolution, give by $U(t, t_0) = e^{-i(t-t_0)H/\hbar}$. It follows that if we use a system with a Hamiltonian with the right terms, we can generate squeezed states of light.

2.5 Input Output Theory

Although we can use the formulas from the previous section to examine the nature of squeezing, we need another approach to connect the theory of squeezing to its actual generation in our experiment. We use an optical parametric oscillator (OPO) to generate squeezing. An OPO is an optical cavity with a non-linear medium included in the beam path, so that light fields of different frequencies may be coupled to one another. Like a laser cavity, OPOs may be operated above or below a threshold (an OPO below threshold is often called an optical parametric amplifier, or OPA). Above threshold, the OPO emits coherent (classical) states of light, so our interest is in an OPO operated below threshold. Our OPO is set up to down-convert photons of green 532 nm light supplied by a laser (known as the pump beam) into two photons of IR 1064 nm "signal" light. The amount of squeezing in the OPO's output beams is determined by the strength of the pump beam, the losses in the OPO, the transmission of the output coupler, and the strength of the non-linear interaction [17].

We will describe our cavity with a Hamiltonian of the form[17]

$$H_{tot} = H_{sys} + H_b + H_{int} \tag{42}$$

Here H_{sys} represents the internal modes of the cavity, H_b the external input and output fields (the b stands for bath), and H_{int} the coupling between the intra-cavity modes and the external fields. In the following analysis, a will refer to the internal modes of the field, and $a_{in,out}$ to the external fields. The internal/external modes simply refer to the modes of light that exist inside and outside the optical cavity, respectively.

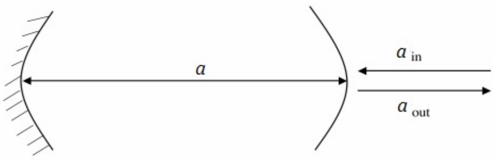

Figure 1: A model of an optical cavity with internal mode a, and external modes at only one port. [18]

The equation (using the interaction picture) for the internal field operators becomes

$$\frac{da}{dt} = -\frac{i}{\hbar}[a, H_{sys}] - \frac{\gamma}{2} + \gamma' a_{in} \tag{43}$$

Here, γ represents the coupling between the internal and external fields, which accounts for the influce of H_b on the internal dynamics of the cavity. Due to the boundary conditions at the mirrors, $\gamma' = k\gamma$. Here, k is derived from the the continuity of the boundary conditions at the mirror. Using time reversal symmetry, we can write the system of equations [17]

$$\begin{aligned}\frac{da}{dt} &= -\frac{i}{\hbar}[a, H_{sys}] - \frac{\gamma}{2} + \gamma' a_{in} \\ &= -\frac{i}{\hbar}[a, H_{sys}] + \frac{\gamma}{2} - \gamma' a_{out}\end{aligned} \tag{44}$$

By solving these equations and eliminating the internal field operators, we can see the relationship between the input and output fields directly. As these equations form a linear system, we can simplify them into the form [17]

$$\begin{aligned}\frac{d\vec{a}}{dt} &= [\underline{A} - \frac{\gamma}{2}\underline{I}]\vec{a} + k\gamma\vec{a}_{in} \\ &= [\underline{A} + \frac{\gamma}{2}\underline{I}]\vec{a} - k\gamma\vec{a}_{out}\end{aligned} \tag{45}$$

Where $\vec{a}$ is

$$\vec{a} = \begin{bmatrix} a \\ a^{\dagger} \end{bmatrix} \tag{46}$$

and $\underline{\mathrm{I}}$ is the identity matrix, and $\underline{\mathrm{A}}$ is the matrix that determines our system of equations. We now examine our operator as a function of frequency

$$\tilde{a}(\omega) = \frac{1}{\sqrt{2\pi}}\int_{-\infty}^{\infty} e^{-i\omega t} a(t) dt \tag{47}$$

Taking into account frequency, we write rewrite Eq. (36) as

$$\begin{aligned}-i\omega\tilde{\vec{a}} &= [\underline{A} - \frac{\gamma}{2}\underline{I}]\tilde{\vec{a}} + k\gamma\tilde{\vec{a}}_{in} \\ &= [\underline{A} + \frac{\gamma}{2}\underline{I}]\tilde{\vec{a}} - k\gamma\tilde{\vec{a}}_{out}\end{aligned} \tag{48}$$

We can now solve this system to eliminate the internal mode, and obtain the output mode in terms of the input mode, which is what we are interested in. Doing this yields [17]

$$\tilde{\vec{a}}_{out} = [\underline{A} + (\frac{\gamma}{2} + i\omega)\underline{I}][-\underline{A} + (\frac{\gamma}{2} - i\omega)\underline{I}]^{-1}\tilde{\vec{a}}_{in} \tag{49}$$

In the next section, we will apply this equation to the OPO specifically.

2.6 The input-output theory of the OPO

Now, let us examine the case of the degenerate OPO (in which the two signal photons are in the same mode) first. This will give us a single mode squeezed state. For a degenerate OPO below threshold, the Hamiltonian will take the form

$$H_{sys} = \hbar\omega_0 a^{\dagger} a + \chi\frac{1}{2}i\hbar[a_p(a^{\dagger})^2 - a_p^{\dagger}a^2] \tag{50}$$

The grouping of operators represents the conversion of one pump photon into two signal photons, and the conjugate process. χ is the nonlinear coupling of our process. In order for this interaction to occur, the down-converted frequency ω_0 must be exactly half the pump frequency. Now let's assume that we have an undepleted pump, or that the pump is in a classical state which remains unchanged with respect to the relatively small number of photons that are converted into signal light. This allows us to write the pump operators as $a_p = \epsilon e^{-i\omega t}$, with ω_p as the pump frequency and ϵ as the pump intensity. We can now re-write the Hamiltonian [17]

$$H_{sys} = \hbar\omega_0 a^\dagger a + \frac{1}{2} i\hbar[\epsilon e^{-i\omega_p t}(a^\dagger)^2 - \epsilon^* e^{i\omega_p t} a^2] \tag{51}$$

In this equation, the coupling constant χ has been folded into the effective amplitude of the pump. Notice that the second half of this Hamiltonian now has the form required to act as the squeezing operator $S(\xi)$. Now if we transform our operators into the rotating frame so that $a \rightarrow ae^{i\omega_p t}$, we get the matrix equation [17]

$$\frac{d\vec{a}}{dt} = [\underline{A} - \frac{1}{2}(\gamma_1 + \gamma_2)\underline{I}]\vec{a} + \sqrt{\gamma_1}\vec{a}_{in} + \sqrt{\gamma_2}\vec{b}_{in} \tag{52}$$

where the matrix is

$$\underline{A} = \begin{bmatrix} 0 & \epsilon \\ \epsilon^* & 0 \end{bmatrix} \tag{53}$$

and the extra operator b and coefficient γ_2 represent that we now have a two sided cavity, with γ_2 accounting for the interactions at the second mirror. This means that our state can couple to external modes through more than one mirror. Although the OPO used in this experiment is intended to function as a one-sided cavity, second output mode can be used to keep track of losses through mirrors other than the output coupler.

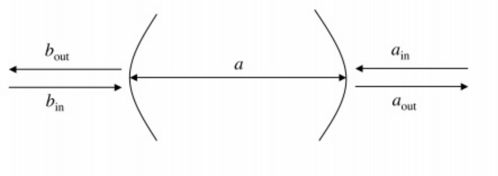

Figure 2: A two sided cavity may have inputs and outputs at two mirrors, so there are more fields to keep track of[18]. The second input/output is often used to keep track of losses, in which case we only look at a_{out} as our desired signal.

While this adds some complication to the algebra, it does not fundamentally change the approach. Using Eq (49), we can now calculate the output field. After substituting in the correct matrix, we ultimately arrive at [19]

$$\begin{aligned} a_{out}(\omega_0+\omega) = {} & \frac{[(\frac{1}{2}\gamma_1)^2 - (\frac{1}{2}\gamma_2 - i\omega)^2 + |\epsilon|^2]a_{in}((\omega_0+\omega) + \epsilon\gamma_1 a^\dagger_{in}((\omega_0-\omega)}{(\frac{1}{2}\gamma_1 + \frac{1}{2}\gamma_2 - i\omega)^2 - |\epsilon|^2} \\ & - \frac{\sqrt{\gamma_1\gamma_2}(\frac{1}{2}\gamma_1 + \frac{1}{2}\gamma_2 - i\omega)b_{in}(\omega_0+\omega) + \epsilon\sqrt{\gamma_1\gamma_2}b^\dagger_{in}(\omega_0-\omega)}{(\frac{1}{2}\gamma_1 + \frac{1}{2}\gamma_2 - i\omega)^2 - |\epsilon|^2} \end{aligned} \tag{54}$$

Using the output field, we can calculate the quadrature variances, and the squeezing spectrum in terms of the output frequency [19]. The maximum output squeezing occurs when $|\epsilon| = \frac{1}{2}(\gamma_1 + \gamma_2)$, which relates the pump power and the reflectivity of the OPO mirrors. This relation also gives the threshold power of the OPO.The setup in this paper is most accurately represented by the single sided cavity (with small losses), so $\gamma_2 \ll \gamma_1$. The other parameters are a vacuum input, and pump power near threshold. Let $\gamma_1 + \gamma_2 = \gamma$. We can derive the following formulas for the variance of the quadrature outputs [18]

$$\begin{aligned} V_{X,out} &= \frac{\omega^2 + (\frac{\gamma}{2})^2 + |\epsilon|^2 + \epsilon\gamma - \gamma_1\gamma_2}{\omega^2 + (\frac{\gamma}{2})^2 + |\epsilon|^2 - \epsilon\gamma} \\ V_{P,out} &= \frac{\omega^2 + (\frac{\gamma}{2})^2 + |\epsilon|^2 - \epsilon\gamma + \gamma_1\gamma_2}{\omega^2 + (\frac{\gamma}{2})^2 + |\epsilon|^2 + \epsilon\gamma} \end{aligned} \tag{55}$$

Now let $d = \frac{|\epsilon|}{\frac{\gamma}{2}}$, and recall that $\gamma_2 \ll \gamma$. We can re-write the output quadrature variances as [18]

$$\begin{aligned} V_{X,out} &= 1 + (\frac{\gamma - \gamma_2}{\gamma})\Big(\frac{4d}{4(\frac{\omega}{\gamma})^2 + (d-1)^2}\Big) \\ V_{P,out} &= 1 - (\frac{\gamma - \gamma_2}{\gamma})\Big(\frac{4d}{4(\frac{\omega}{\gamma})^2 + (d+1)^2}\Big) \end{aligned} \tag{56}$$

This shows that $V_{X,out} > 1$ and $V_{P,out} < 1$ so the corresponding output quadratures are anti-squeezed and squeezed respectively (in this calculation, the variances are scaled so that $V < 1$ gives squeezing). We could also use this formula to calculate how much squeezing is to be expected if we measure all the parameters of our system. It is also possible to calculate the squeezing level for a non-degenerate OPO, which is governed by the Hamiltonian

$$H_{sys} = \hbar\omega_0 a_1^\dagger a_1 + \hbar\omega_0 a_2^\dagger a_2 + \frac{1}{2}i\hbar[\epsilon e^{-i\omega_p t} a_1^\dagger a_2^\dagger - \epsilon^* e^{i\omega_p t} a_1 a_2] \tag{57}$$

in which modes a_1 and a_2 denote different frequencies. In this case we derive a result through a similar process (omitting tedious algebra) [20]

$$V_{TMS} = 1 - \frac{8\gamma_{nl}^2 - 8\gamma_{nl}\gamma(V_{laser} - 1)}{(3\gamma_{nl} + \gamma)^2 + \omega^2} \tag{58}$$

in which $\gamma_{nl} = \frac{|\epsilon|^2}{2\gamma}$ and V_{laser} is the classical noise of the laser. Again, we can see that this can be less than one, giving a squeezed result. This variance is that of the two mode quadrature, described in equations 36 and 37.

2.7 Optical Frequency Comb

The output of an OPO will take the form of an optical frequency comb. First, if we label the pump frequency as ω_p, then our two photons must satisfy the condition

$\omega_1 + \omega_2 = \omega_p$ in order to conserve energy. Second, the frequencies of all three photons must work with the phase-matching bandwidth of our OPO, which has been measured to be 3.2 THz [10]. Third, due to the resonant enhancement of the cavity, the output photons will be overwhelmingly emitted in the resonant cavity modes of the OPO. These modes are separated in frequency by the free spectral range (FSR) of the OPO; ours has an FSR of .95 GHz [10]. These two properties, the phase-matching bandwidth of the crystals and FSR of the OPO determine the size and the spacing of the QOFC. When we have the possibility of many modes being produced instead of just two, we rewrite our Hamiltonian in sum form [10].

$$H = i\hbar \sum_{i=0}^{N} \kappa_i a_i^\dagger a_{-i}^\dagger + H.C. \tag{59}$$

Here, κ takes into account the pump power and non-linear coupling coefficient(and anything else affecting the strength of the interaction).The subscripts are labeled so that the pump frequency is at i=0 and the integers label by how many FSRs the corresponding modes are separated. Solving the Heisenberg equations for the creation/annihilation operators and translating these results into the quadrature operators p and q shows that this Hamiltonian will produce two-mode, quadrature squeezed states of light.

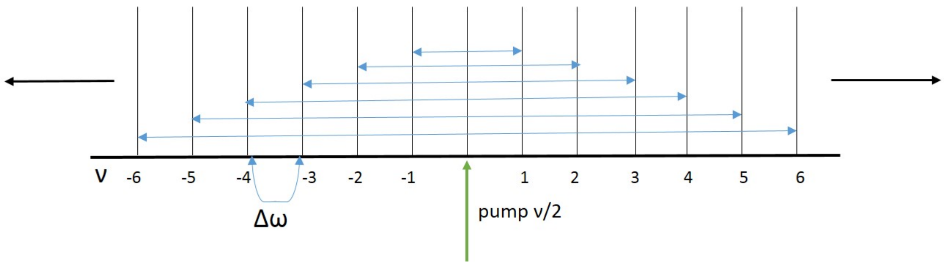

Figure 3: The optical frequency comb as formed by a single pump. The vertical lines represent modes of the OPO. The vertical arrow shows half the pump frequency and the horizontal arrows connect modes which form entangled pairs.

Although previous work in the lab has focused on using the building block of the optical frequency comb to create states with more complex entanglement structure, my thesis does not focus on those efforts.

2.8 Homodyne Detection

This section is based on analysis in *Introductory Quantum Optics* by Knight and Gerry [16]. It is not trivial to measure the quadrature operators of a light mode directly. While photon counting detectors do exist, most work of this kind, including in our lab, is done with photodiodes. Photodiodes provide a measurement of the intensity of the light field, $I = \langle a^\dagger a \rangle$. In order to measure the quadratures of our light, we need a beamsplitter, and an electronic subtraction circuit. In quantum optics, beam splitters provide the following relationship between their input modes a,b and output modes c,d

$$\begin{aligned} c &= t'a + rb \\ d &= r'a + tb \end{aligned} \tag{60}$$

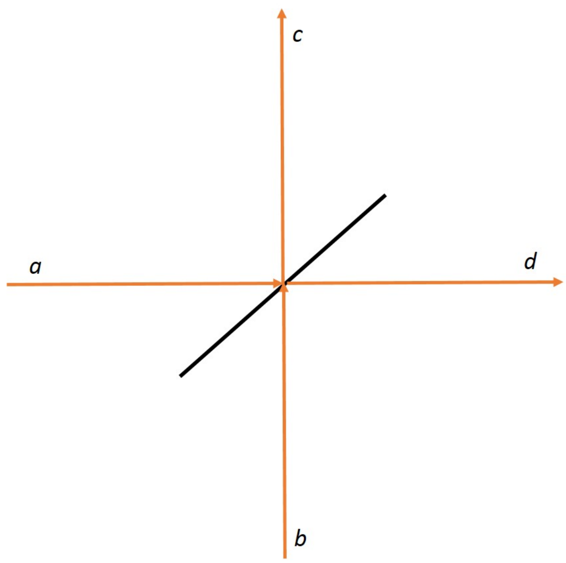

Figure 4: A beam-splitter [15]

In order to conserve photon number and preserve unitarity (we assume the beam-splitter to be lossless), r and t follow the conditions

$$\begin{aligned} |r| = |r'|, |t| &= |t'| \\ |r|^2 + |t|^2 &= 1 \\ r^* t' + r' t^* &= 0 \\ r^* t + r' t'^* &= 0 \end{aligned} \tag{61}$$

We use the following setup in experiment with a balanced beamsplitter. In the case of a balanced beam splitter

$$\begin{aligned} c &= \frac{1}{\sqrt{2}}(a + ib) \\ d &= \frac{1}{\sqrt{2}}(ia + b) \end{aligned} \tag{62}$$

In order to measure the quadrature operators with only intensity measurements, we must use a technique called homodyne detection. We place photodetectors at each output port of beamsplitter and electronically subtract their signals

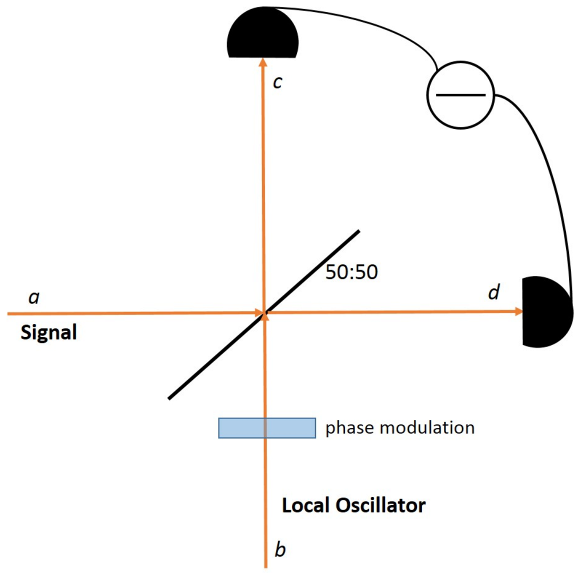

Figure 5: The balanced homodyne measurement. [15]
This setup is what was used obtaining the results of this thesis.

This gives us

$$\begin{aligned} I_c - I_d &= \langle c^\dagger c - d^\dagger d \rangle \\ &= i\langle a^\dagger b - ab^\dagger \rangle \end{aligned} \tag{63}$$

Now assume one of our inputs is in a coherent state (this is known as the local oscillator) $\left|\beta e^{-i\Phi} e^{-i\omega t}\right\rangle$ so we can write $b = |\beta| e^{-i\Phi} e^{-i\omega t}$ which gives us

$$I_c - I_d = |\beta|(ae^{i\omega t}e^{-i\theta} + a^\dagger e^{-i\omega t}e^{i\theta}) \tag{64}$$

Where $\theta = \Phi + \pi/2$. The input that is in a coherent state is known as the local oscillator. Now, if a is at the same frequency as b, we can cancel the time dependent terms, and we are left with

$$I_c - I_d = 2|\beta|[\frac{1}{2}(ae^{-i\theta} + a^\dagger e^{i\theta})] = 2|\beta| X(\theta) \tag{65}$$

This $X(\theta)$ is a general quadrature operator, and can be tuned from X to P by tuning the relative phases of the local oscillator and signal beam. In this way, we can directly measure the quadrature operators of an unknown state of light.

2.9 Intra-Mode Squeezing

Let us now examine a case where our squeezed signal has a relatively wide bandwidth, and the local oscillator has two narrow frequencies (we can treat them as delta functions in frequency compared to the squeezed mode). We will refer to such an arrangement as a bichromatic local oscillator, or BLO. The central frequency of the broadband light is ω_0 and the two local oscillator frequencies are $\omega_0 \pm \Omega_0$. The difference in photo-currents in our homodyne measurement analyzed at a specific radio frequency Ω is [14]

$$I(\Omega) = \frac{1}{\sqrt{2}}[a(\Omega_0-\Omega)+a(-\Omega_0-\Omega)]e^{-i\theta}+\frac{1}{\sqrt{2}}[a^\dagger(\Omega_0+\Omega)+a^\dagger(-\Omega_0+\Omega)]e^{i\theta} \quad (66)$$

Where we have ignored the constant that arises from the coherent state. This equation derives from (63) by simply assuming that the inputs to our homodyne beam splitter are a linear combination of modes at frequencies $\omega_0 \pm \Omega$. The quantity Ω_0 is the separation of the two frequencies we use in the bichromatic local oscillator. If we let the quadratures of the signal field be X and P, then we can define the following

$$\begin{aligned} X_B(\Omega) &= \frac{1}{\sqrt{2}}[X(|\Omega_0 - \Omega|) + X(-\Omega_0 + \Omega)] \\ P_B(\Omega) &= \frac{1}{\sqrt{2}}[P(|\Omega_0 - \Omega|) + P(-\Omega_0 + \Omega)] \end{aligned} \quad (67)$$

The two frequency terms result from measuring symmetrically with our BLO. Now, it remains to be shown what properties the sidebands which exist in this broadband squeezed light mode will have.

We can in fact break down a single broadband squeezed light mode into multiple EPR pairs of modes in general [12]. In more general notation, the signal field's quadrature may be written as

$$X(\Omega, \theta) = \frac{1}{\sqrt{2}}[a(\omega_0 - \Omega)e^{-i\theta} + a^\dagger(\omega_0 + \Omega)e^{i\theta}] \quad (68)$$

where ω_0 is the central frequency of the signal light. Here we assume that we have squeezing such that

$$\begin{aligned} \Delta X &= e^{-2r} < 1 \\ \Delta P &= e^{2r} > 1 \end{aligned} \quad (69)$$

By treating the upper and lower sidebands as separate modes, and using a beamsplitter transformation to separate them, we can arrive at modes which satisfy the equations [12]

$$\Delta X(\omega_0 + \Omega) = \Delta X(\omega_0 - \Omega) = \Delta P(\omega_0 + \Omega) = \Delta P(\omega_0 - \Omega) = \frac{e^{2r} + e^{-2r}}{2} > 1 \quad (70)$$

for the individual quadratures, but for the sums we have

$$\Delta[X(\omega_0 + \Omega) - X(\omega_0 - \Omega)]/2 = \Delta[P(\omega_0 + \Omega) + P(\omega_0 - \Omega)]/2 = e^{-2r} < 1 \quad (71)$$

and for the conjugate operators

$$\Delta[X(\omega_0 + \Omega) + X(\omega_0 - \Omega)]/2 = \Delta[P(\omega_0 + \Omega) - P(\omega_0 - \Omega)]/2 = e^{2r} > 1 \quad (72)$$

These are the conditions for two mode squeezing, and this is what we will attempt to measure in our experiment, the squeezing between two sidebands of broadband squeezed light.

3 Experimental Principles

Our experiment uses an OPO with a four mirror bow-tie cavity configuration, which houses two periodically poled $KTiOPO_4$ (KTP) crystals. Spontaneous parametric down conversion (SPDC) of a single 532 nm wavelength pump photon into two 1064 nm photons can occur in each crystal. Our crystals are identical, both being x-cut. They are oriented at 90° from each other, so that one allows for a zzz polarized process and the other for yyy. In the results of this thesis, only the zzz polarized process was used, so we used only the z polarized, pump beam.

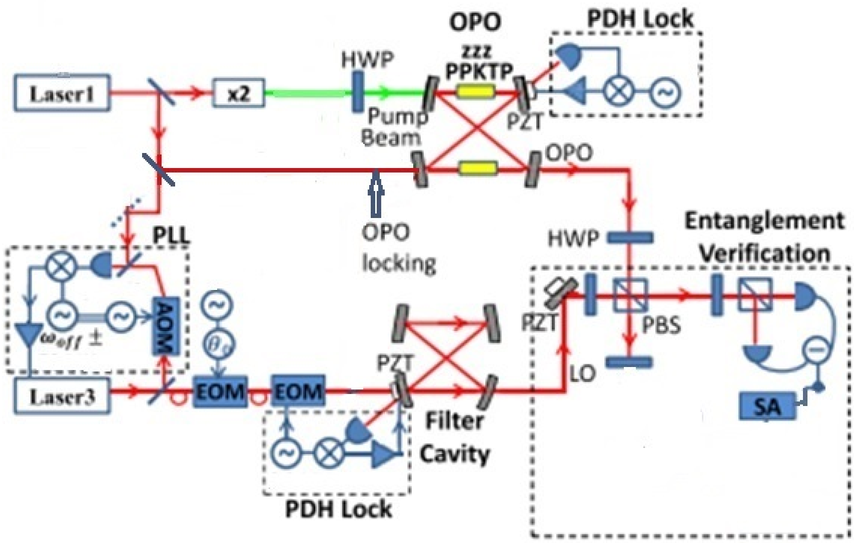

Figure 6: A diagram of the optical setup used in this thesis.

In order to measure squeezing, several conditions must be satisfied. The pump beam must be phase locked to the local oscillator. Our pump laser (L1) is an ultrastable continuous-wave Nd:YAG laser [15] ("Diabolo" by Innolight) with an internal doubling cavity that emits green light in addition to the generated IR. The laser that provides our local oscillator (L3) is another CW Nd:YAG laser (JDSU Ligtwave Electronics Model 126) [15]. The two lasers are phase-locked to one another using a 70 MHz beatnote. The beam from L3 passes through an acousto-optical modulator (AOM) which has an electronic signal of 70 MHz feeding it. The resulting shifted beam is combined with light from L1 on a beam splitter, and the interference is used to phase lock the two lasers. Locking the beam from L1 to the shifted beam of L3 at a difference of 70 MHz compensates for the shift, and locks the output of the two lasers at the same frequency. This is done by comparing the beatnote to an electronic 70 MHz signal. This technique is useful because a beatnote of some kind is helpful to lock, so the frequency difference cannot be zero between two beams.

The pump laser must also be mode-locked to the OPO cavity itself, which we accomplish using the Pound-Drever-Hall (PDH) locking technique. The IR output from the pump laser is modulated at 12 MHz, and this signal is used to lock the OPO.

Now, in order to measure two mode squeezing within a single mode of the OPO, we need a bichromatic local oscillator with two closely spaced frequencies. We accomplish this by using a fiber coupled EOM and a filter cavity. The local oscillator light from L3 is PDH locked to the filter cavity using a modulation of 9.17 MHz.

In order to generate the bichromatic local oscillator, we engineered an electronic signal using an RF mixer, combining a 700 MHz LO signal and an IF frequency ranging from 50 to 800 kHz. The resulting signal has two frequencies present.

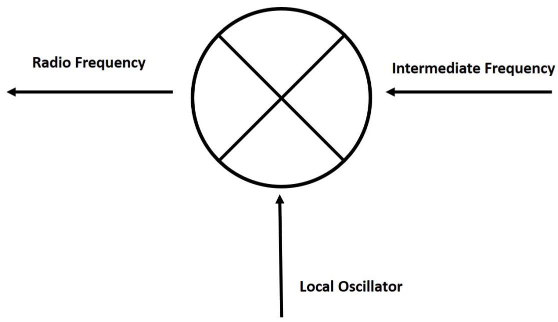

Figure 7: An electronic frequency mixer used in the up-conversion mode. The local oscillator is an electronic RF freqency (not to be confused with the homodyne beam), the intermediate frequency is kHz range, and the RF is the output with $f_{RF} = f_{LO} \pm f_{IF}$.(information from Digikey's website, an article titled "The Basics of Mixers")

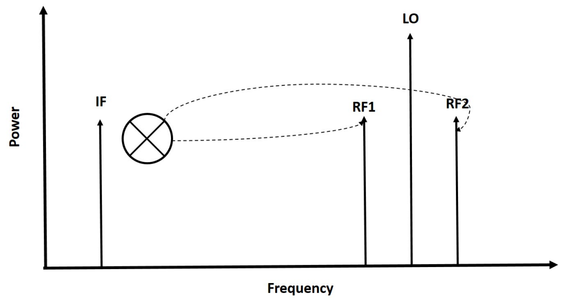

Figure 8: The frequency picture of the electronic mixer. The two RF outputs are centered around the local oscillator, but some power from the LO and the IF always leaks through.(information from Digikey's website, an article titled "The Basics of Mixers")

When applied to an EOM, it modulates the light so that four sidebands are created. Modulation with an EOM creates two sidebands symmetrically around the carrier frequency, so modulating with two signals simultaneously produces a total of five frequencies.

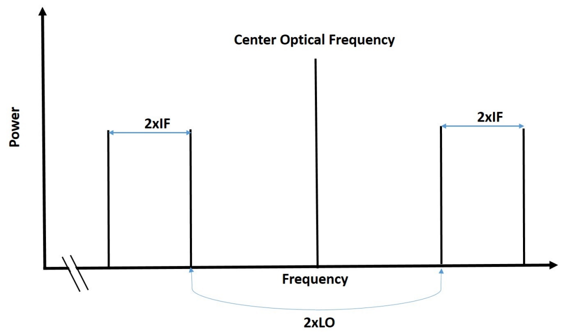

Figure 9: The frequency structure of the optical local oscillator, showing each pair of sidebands is separated by $2f_{IF}$ and the two pairs are separated by $2f_{LO}$.

Now, by PDH locking our modulated light to a filter cavity (which has the same properties as the OPO, but lacks non-linear crystals) we can choose to keep either pair of sidebands, or the carrier frequency. Each sideband pair is close enough so that the 10 MHz bandwidth of the filter cavity will pass it easily, but the two sideband pairs and the central frequency are separated by enough so that the filter cavity will exclude the undesired components. This technique allows us to flexibly create a bichromatic local oscillator, or BLO.

4 Results

4.1 Squeezing at Various BLO separations

In order to verify intra-mode squeezing, and confirm the scalability of the technique, we measured squeezing using the bichromatic local oscillator with various frequency spacings. The following plot is an example of the data we took. These traces show the noise level of various optical signals, taken with a spectrum analyzer.

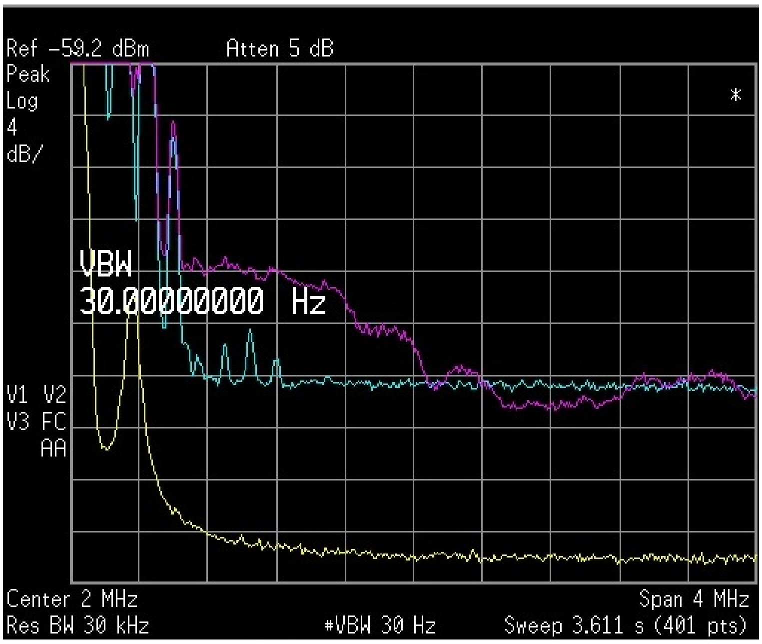

Figure 10: This picture was taken with a 50 kHz sideband separation on the BLO. Squeezing is typically measured in dB, according to the formula $S(dB) = 20\log\left(\frac{\text{shot noise level}}{\text{squeezed noise level}}\right)$. Every squeezing trace in this uses one box as 4 dB on the vertical scale. Other information on the vertical and horizontal scales is included in the screenshot.

In all squeezing images in this section, the lower (yellow) trace is the electronics noise of the detectors, the sky blue trace is the noise of the coherent state local oscillator (measured by blocking the quantum light), and the purple trace is the squeezed signal. The level of the shot noise is determined by the power of the local oscillator, as the variance of a coherent state is related to its expected photon number. When the noise of the squeezed signal drops below the shot noise, it means that the relative phases of the local oscillator and signal are so that we measure the squeezed quadrature. When it is higher, it means that we are measuring the anti-squeezed quadrature. Squeezing does not appear over the entire trace because of fluctuations in path length for the two beams that cannot be compensated for with a phase lock. The squeezing level that appears here is approximately 2.5-3 dB, which remains fairly constant across the different BLO separations.

The following figures show the squeezing level for increasing BLO separation.

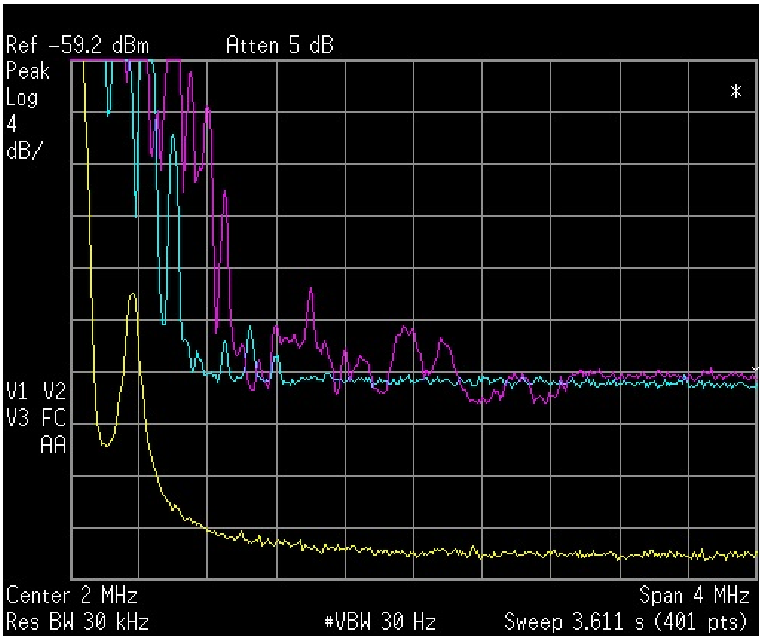

Figure 11: This picture was taken with a 75 kHz sideband separation on the BLO.

In this trace, the noise in the lower fourth of the spectrum is even more apparent. This is due to the electronic mixing that is used to create the sidebands. The RF mixer always some of the LO signal to pass, so the laser is modulated at 75 kHz, and multiples of that due to harmonics. The harmonics could be eliminated by using a lower electronic power, but then the EOM was not modulated strongly enough. If the frequency of the LO input is low enough, this modulation is buried in the low frequency noise of the detection (which comes from the detector electronics). However, if the frequency is high enough, these modulation peaks on the local oscillator interfere with the squeezing measurement.

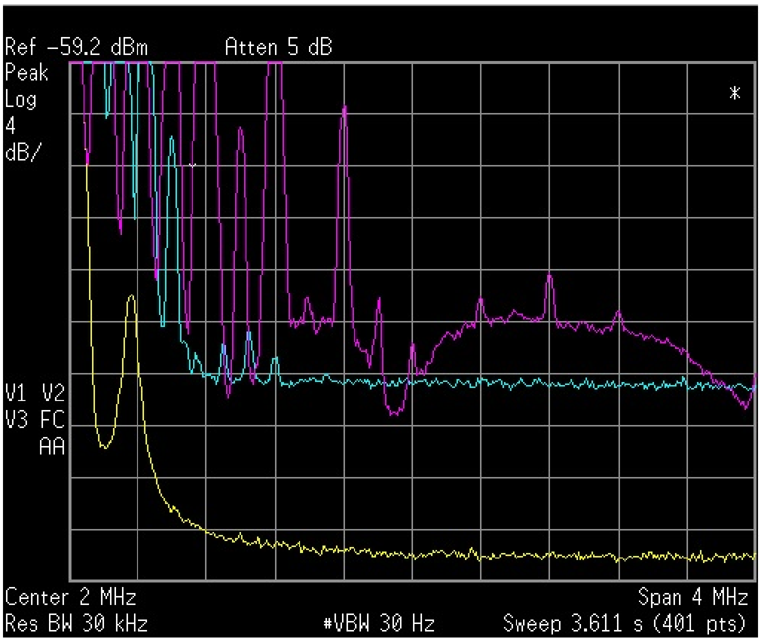

Figure 12: This picture was taken with a 100 kHz sideband separation on the BLO.

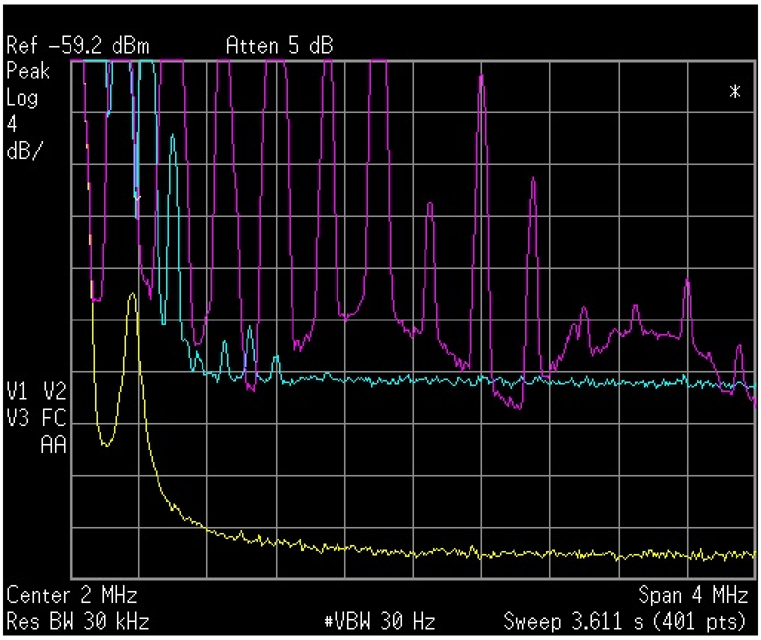

Figure 13: This picture was taken with a 200 kHz sideband separation on the BLO.

In the previous two figures, the modulation peaks have become much more apparent. In the 200 kHz trace, the squeezing is barely visible (only around 2.5

MHz does the noise level drop below shot noise). For future squeezing traces, a change of measurement technique was necessary.

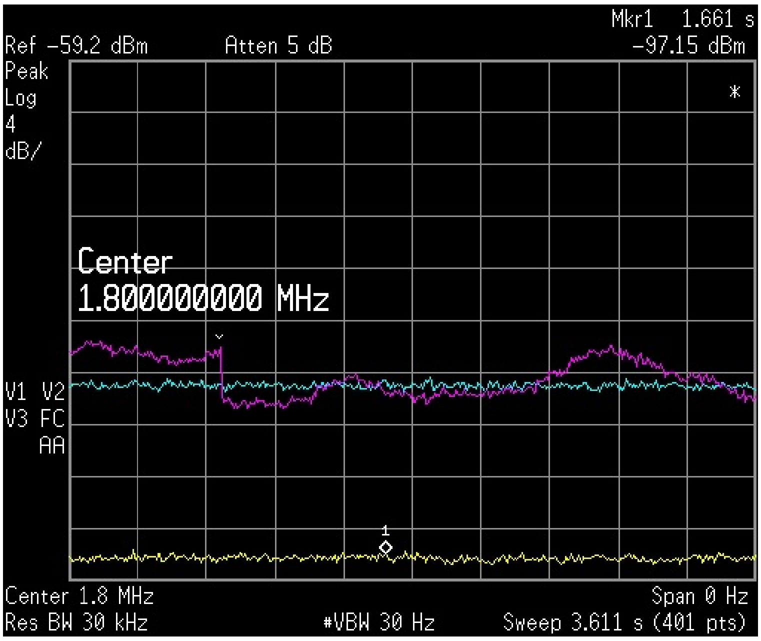

Figure 14: This picture was taken with a 300 kHz sideband separation on the BLO. The x axis is now in time, and it simply records the noise level at a particular frequency over the sweep time. This is the case for all zero span spectrum analyzer traces in this thesis.

On this trace, and all remaining squeezing measurements, we used the zero span measurement on our spectrum analyzer. This allows us to examine only the location on the squeezing trace where squeezing is visible. The noise fluctuations on these traces still represent the relative phase shift of the quantum light and local oscillator.

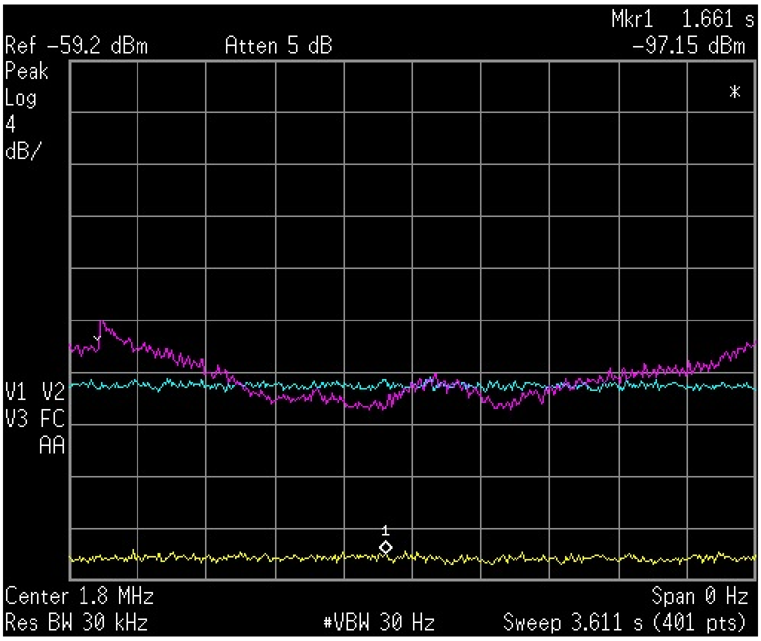

Figure 15: This picture was taken with a 400 kHz sideband separation on the BLO.

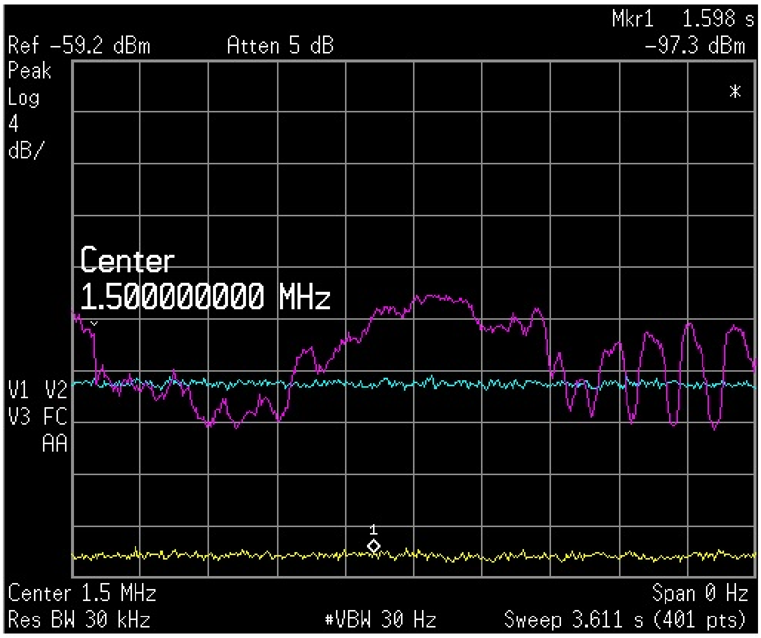

Figure 16: This picture was taken with a 500 kHz sideband separation on the BLO.

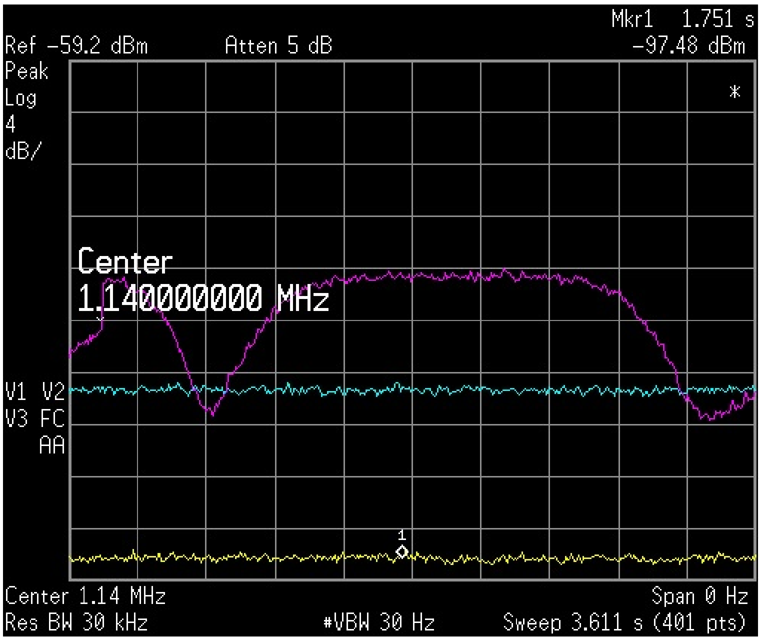

Figure 17: This picture was taken with a 600 kHz sideband separation on the BLO.

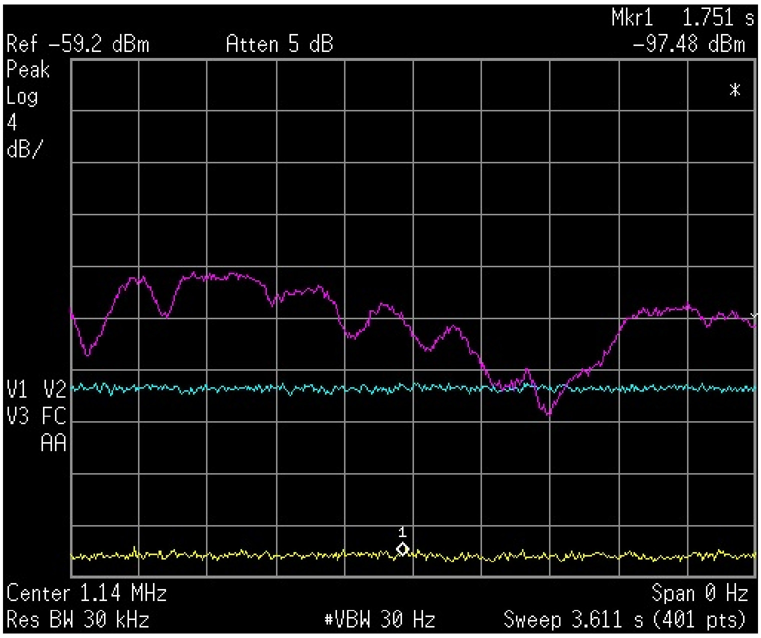

Figure 18: This picture was taken with a 700 kHz sideband separation on the BLO.

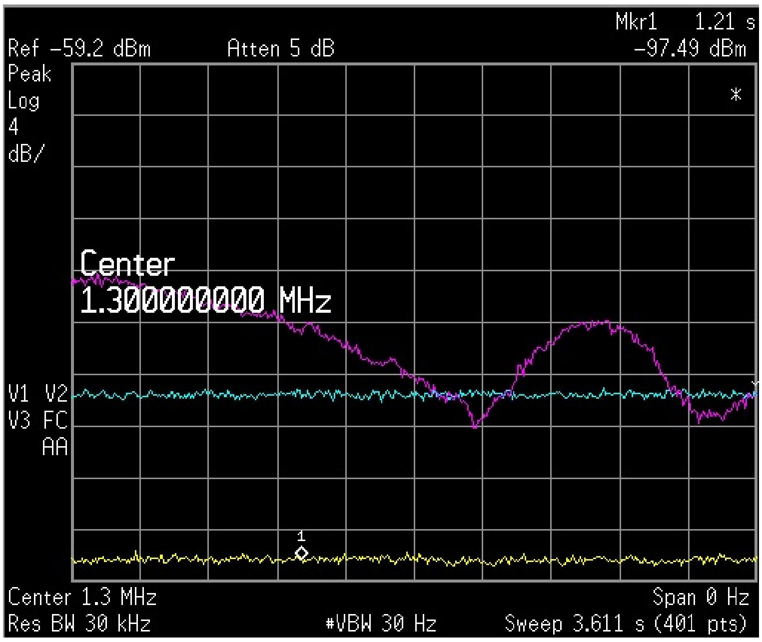

Figure 19: This picture was taken with an 800 kHz sideband separation on the BLO.

As is apparent from these figures, the squeezing level remains consistent for greater shifts of the BLO. We would expect to begin to see a drop in the squeezing level at some point, as the OPO mode has a bandwidth of approximately 10 MHz.

4.2 Disappearance of Squeezing for off center measurements

When measuring squeezing, it is important to confirm that the squeezing disappears when looking at modes that should not be correlated. In this section, we examine squeezing traces which were taken with the entire BLO setup shifted off center, so that its two frequencies were no longer located symmetrically about the frequency of the OPO mode. As the shift increases, the two sidebands should no longer be addressing modes which have any quantum correlations, and this is in fact the result. Each measurement here is taken with a BLO width of 50 kHz.

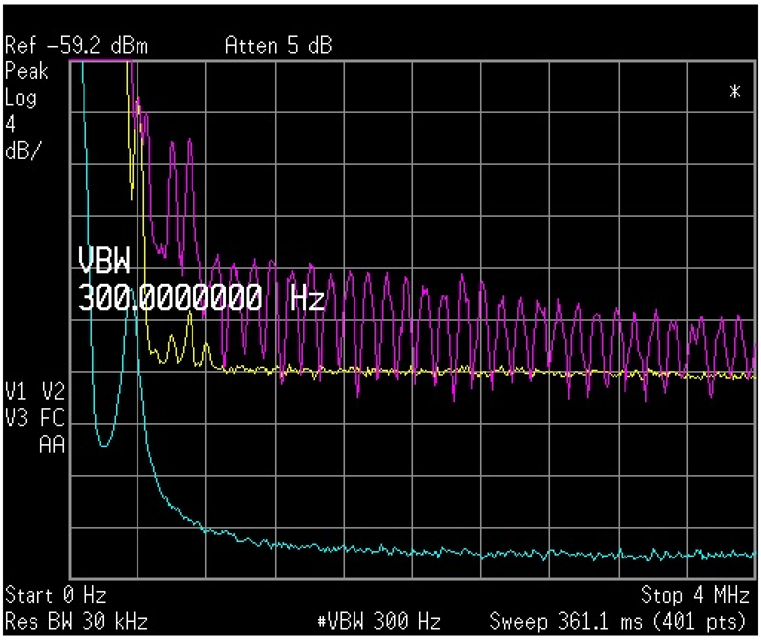

Figure 20: This trace was taken with a 50 Hz shift from the central frequency.

Although squeezing is still present in this trace, it is starting to be canceled out by beatnote oscillations between the local oscillator and the squeezed signal. We tried to avoid under-sampling the data by increasing the video bandwidth of the spectrum analyzer. The squeezing should be completely gone as we shift outside the bandwidth of our local oscillator, which is less than 1 kHz.

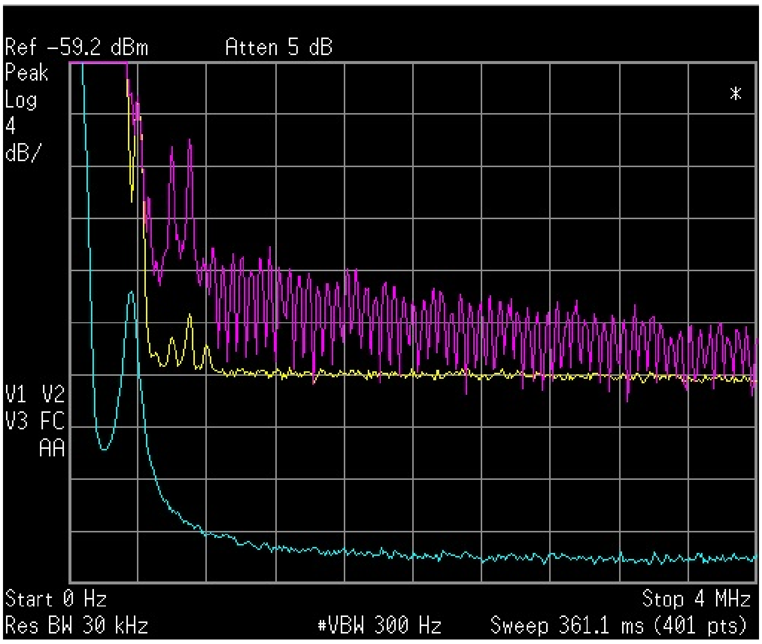

Figure 21: This trace was taken with a 100 Hz shift from the central frequency.

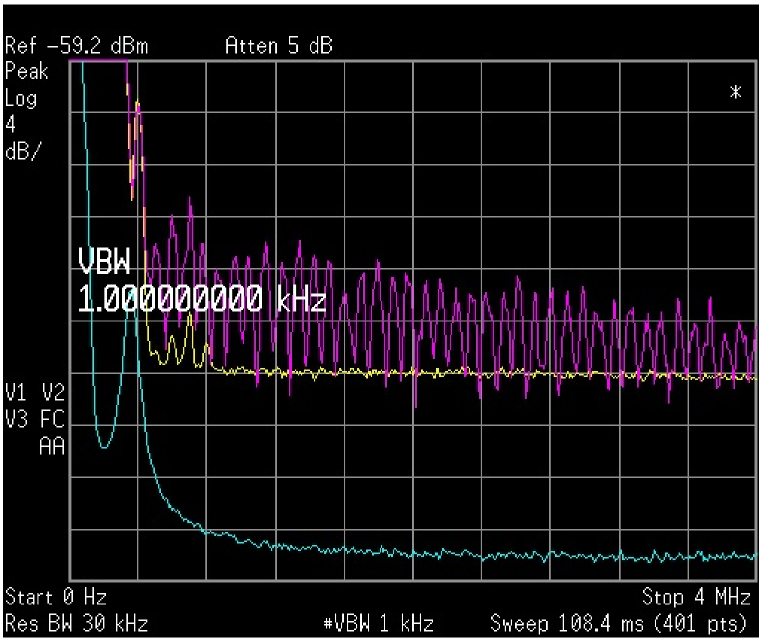

Figure 22: This trace was taken with a 200 Hz shift from the central frequency.

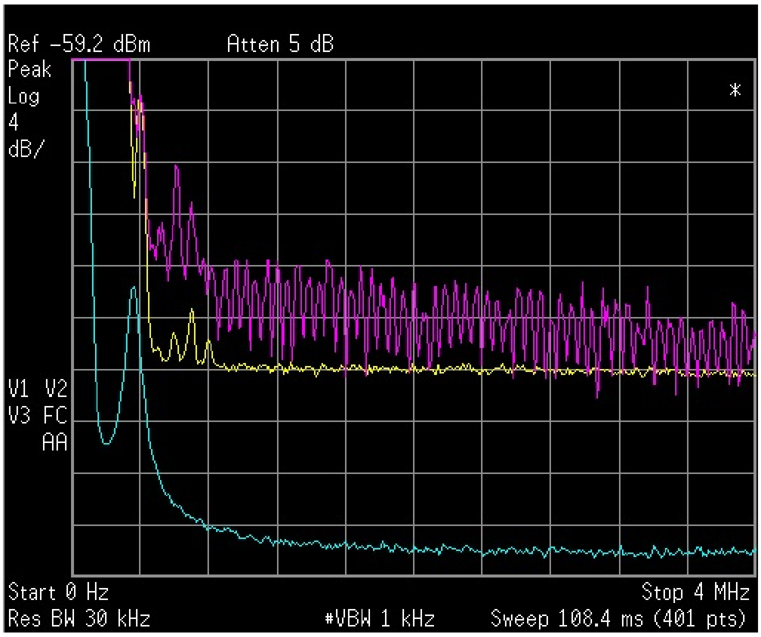

Figure 23: This trace was taken with a 300 Hz shift from the central frequency.

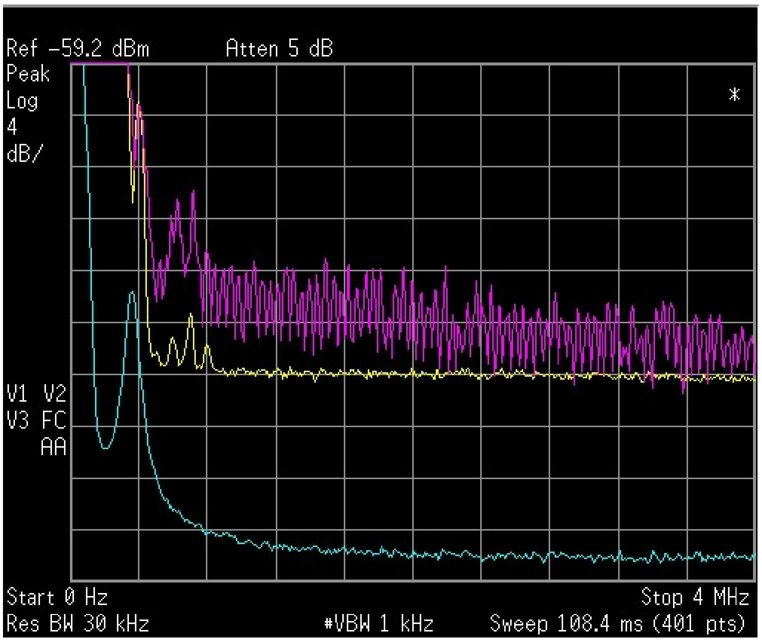

Figure 24: This trace was taken with a 400 Hz shift from the central frequency.

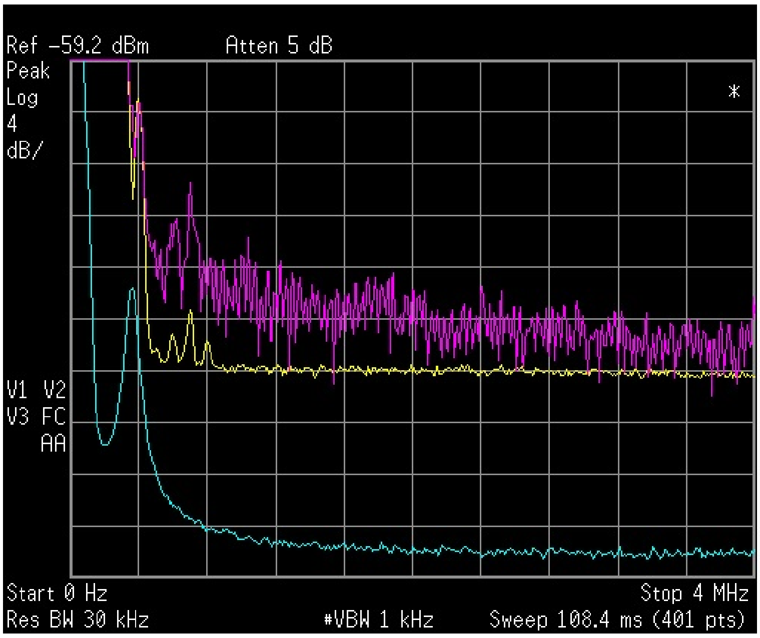

Figure 25: This trace was taken with a 500 Hz shift from the central frequency.

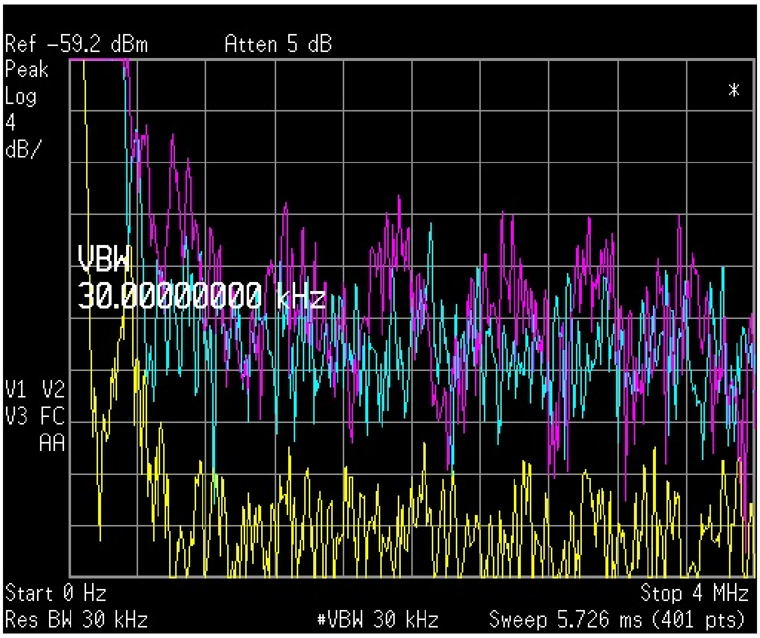

Figure 26: This trace was taken with a 600 Hz shift from the central frequency. On this trace, the size of the oscillations are beginning to make it harder to see the squeezing. The VBW of the spectrum analyzer had to be increased for this trace, resulting in a noisier spectrum.

These traces confirm the squeezing disappears as we shift our LO away from the center of the broadband squeezed mode. This confirms that our quantum correlations have the structure we expected to observe. It is important to note how quickly the squeezing disappears; qualitatively, it starts to fade away at an approximately 1 kHz shift. This is in contrast to the centered case, in which each sideband was displaced from the center by at least 50 kHz. This helps show that we are not simply measuring single mode squeezing with our BLO, but actually a two mode effect.

5 Conclusions

In Conclusion, we have demonstrated a technique for measuring intra-mode entanglement in the output squeezing mode of an optical parametric oscillator. It has been shown that a light field with broadband squeezing can be analyzed as a collection of two mode squeezed side band fields arranged around a center frequency. The limit of how narrow the sideband fields may be is only set by the bandwidth of the measurement techniques, and by the pump field itself. In order to measure this two mode squeezing signal, it is necessary to use a two-mode, or bichromatic, local oscillator. We generated such a field using a fiber coupled EOM with a double-frequency modulation. This produces a local oscillator with a widely tunable range of sideband separations, but also does not require multiple optical modulators or phase locks in order to work. Using this experimental setup, we were able to verify the presence of squeezing in our output field in the range from 50 kHz to 800 kHz sideband separation. The squeezing level did not drop significantly when measuring the wider sidebands, and the spectrum should extend out to multiple MHz.

This intra-mode squeezing technique opens up new possibilities by allowing for the production of frequency entangled cluster states which are more densely packed in frequency space. Such states would prove useful as large resources for quantum computing.

References

[1] A. Einstein, B. Podolsky, and N. Rosen. "Can quantum-mechanical description of physical reality be considered complete?" In: *Phys. Rev.* 47 (1935), p. 777.

[2] P. W. Shor. "Algorithms for quantum computation: discrete logarithms and factoring". In: *Proceedings, 35th Annual Symposium on Foundations of Computer Science*. Ed. by S. Goldwasser. Santa Fe, NM: IEEE Press, Los Alamitos, CA, 1994, pp. 124–134.

[3] Richard P. Feynman. "Simulating Physics With Computers". In: *Int. J. Theor. Phys.* 21 (1982), pp. 467–488.

[4] R. Raussendorf and H. J. Briegel. “A one-way quantum computer”. In: *Phys. Rev. Lett.* 86 (2001), p. 5188.

[5] P Walther et al. “Experimental One-Way Quantum Computing”. In: *Nature (London)* 434 (2005), p. 169. DOI: 10.1038/nature03347.

[6] B. P. Lanyon et al. “Universal digital quantum simulation with trapped ions”. In: *Science* 334 (2011), p. 57.

[7] Thomas Monz et al. “14-Qubit Entanglement: Creation and Coherence”. In: *Phys. Rev. Lett.* 106.13 (Mar. 2011), p. 130506. DOI: 10.1103/PhysRevLett.106.130506.

[8] B. P. Lanyon et al. “Experimental Demonstration of a Compiled Version of Shor’s Algorithm with Quantum Entanglement”. In: *Phys. Rev. Lett.* 99.25, 250505 (2007), p. 250505. DOI: 10.1103/PhysRevLett.99.250505.

[9] Nicolas C. Menicucci, Steven T. Flammia, and Olivier Pfister. “One-way quantum computing in the optical frequency comb”. In: *Phys. Rev. Lett.* 101 (2008), p. 130501. DOI: 10.1103/PhysRevLett.101.130501.

[10] Moran Chen, Nicolas C. Menicucci, and Olivier Pfister. “Experimental realization of multipartite entanglement of 60 modes of a quantum optical frequency comb”. In: *Phys. Rev. Lett.* 112 (12 Mar. 2014), p. 120505. DOI: 10.1103/PhysRevLett.112.120505. URL: http://link.aps.org/doi/10.1103/PhysRevLett.112.120505.

[11] Shota Yokoyama et al. “Ultra-large-scale continuous-variable cluster states multiplexed in the time domain”. In: *Nat. Photon.* 7 (2013), p. 982.

[12] Jing Zhang. “Einstein-Podolsky-Rosen sideband entanglement in broadband squeezed light”. In: *Phys. Rev. A* 67.67 (May 2003). DOI: 10.1103/PhysRevA.67.054302.

[13] E. H. Huntington et al. “Demonstration of the spatial separation of the entangled quantum sidebands of an optical field”. In: *Phys. Rev. A* 71 (4 Apr. 2005), p. 041802. DOI: 10.1103/PhysRevA.71.041802. URL: http://link.aps.org/doi/10.1103/PhysRevA.71.041802.

[14] Wei Li, Xudong Yu, and Jing Zhang. “Measurement of the squeezed vacuum state by a bichromatic local oscillator”. In: *Opt. Lett.* 40.22 (Nov. 2015), pp. 5299–5301. DOI: 10.1364/OL.40.005299.

[15] Moran Chen. “Large-Scale Cluster-State Entanglement in the Quantum Optical Frequency Comb”. PhD thesis. University of Virginia, 2015.

[16] Christopher C. Gerry and Peter L. Knight. *Introductory Quantum Optics*. Cambridge University Press, 2005.

[17] M. J. Collett and C. W. Gardiner. “Squeezing of intracavity and traveling-wave light fields produced in parametric amplification”. In: *Phys. Rev. A* 30.3 (Sept. 1984), pp. 1386–1391. DOI: 10.1103/PhysRevA.30.1386.

[18] Daruo Xie. "Generation of bright broadband-squeezed light and broadband quantum interferometry". PhD thesis. University of Virginia, 2007.

[19] Crispin Gardiner and Peter Zoller. *Quantum Noise, A Handbook of Markovian and Non-Markovian Quantum Stochastic Methods with Applications to Quantum Optics*. 3rd. Springer Series in Synergetics. Springer, 2004.

[20] Hans A. Bachor and Timothy C. Ralph. *A Guide to Experiments in Quantum Optics*. Wiley, 2004.